Development of Thomson Scattering Diagnostics for Cathode-Directed Streamer Discharges in Helium

Bolouki, Nima
Department of Electrical and Material Science, Faculty of Engineering Sciences, Kyushu University

Hassaballa, Safwat
Department of Physics, Faculty of Science, Al-Azhar University

Tomita, Kentaro
Department of Electrical and Material Science, Faculty of Engineering Sciences, Kyushu University

Uchino, Kiichiro
Department of Electrical and Material Science, Faculty of Engineering Sciences, Kyushu University

https://doi.org/10.15017/1485123

出版情報：九州大学大学院総合理工学報告. 36 (2), pp.1-5, 2015-02. 九州大学大学院総合理工学府
バージョン：
権利関係：

九州大学大学院総合理工学府報告
第 36 巻 第 2 号 1-5 頁 平成 27 年 2 月

Engineering Sciences Reports, Kyushu University
Vol. 36, No. 2, pp. 1-5, FEB, 2015

Development of Thomson Scattering Diagnostics for Cathode-Directed Streamer Discharges in Helium

Nima BOLOUKI[*1,†] Safwat HASSABALLA[*2] Kentaro TOMITA[*1]
and Kiichiro UCHINO[*1]
[†]E-mail of corresponding author: bolouki.nima.721@m.kyushu-u.ac.jp

(Received December 27, 2014, accepted December 29, 2014)

Laser Thomson scattering diagnostics has been developed for the study of the streamer moving toward the cathode in helium near atmospheric pressure. In order to avoid laser perturbation and obtain sufficient intensity of the Thomson scattering signal, two cylindrical lenses were used to optimize the spot size of a probing laser at a focusing point. At a position of 2 mm from the anode (needle electrode), the electron density and electron temperature were successfully measured to be ~ 10^{18} m^{-3} and ~ 2 eV, respectively, in the initial stage of the primary streamer.

Key words: *Non-thermal atmospheric-pressure plasmas, streamers, laser Thomson scattering diagnostics*

1. Introduction

Atmospheric pressure plasmas produced by pulsed discharges are currently being investigated as an effective source of non-equilibrium plasmas. It is well known that the electrical breakdown near atmospheric pressure is described by streamer theory.[1)] Based on streamer dynamics, the initial stage of electrical breakdown is the development of nonlinear ionization waves, known as streamer discharges or primary streamers, in a non-ionized medium, followed by the creation of a weakly-ionized non-equilibrium plasma.[2)-4)] Then, the streamers cross the gap. This final stage of evolution is also known as a secondary streamer.

In the study of streamers, some reports have dealt with the structures and propagation of streamers. For instance, Ref. 5 measured the development of neon streamers as a function of electric field strength and streamer length. The propagation of air streamers and their dependence on applied voltage, distance between electrodes,[6)] and pressure[7)] have also been investigated. In addition, time-resolved measurements[8)] have been successfully performed. Reference 9 measured and simulated pulsed streamers in three spatial dimensions. Furthermore, spectroscopic studies of streamer discharges have been reported. One of these studies utilized measurements and analyses of the absolute intensities of the second and first negative systems of molecular nitrogen to determine the reduced electric field and electron number density.[10),11)] Also, Ono et al. applied optical diagnostic techniques, such as laser-induced florescence, laser absorption, and optical emission spectroscopy, to measure the densities and temperatures of different active species produced inside the pulsed streamer discharge at atmospheric pressure.[12),13)] However, until the present study there has been no direct measurement of the primary streamer to examine the temporal evolution of electron density (n_e) and electron temperature (T_e).

Measurements of n_e and T_e are important to understand the basic structure of the streamer. Also, for the industrial applications of streamers, the active species generated inside the streamers play key roles. Generation of such species is governed by free electrons inside the plasmas. Therefore, measurements of n_e and T_e are essential to understand the behavior of active species.

Laser Thomson scattering (LTS) has been known as one of the most reliable methods to measure the n_e and T_e of plasmas. Moreover, it provides a high spatial resolution.[14)-19)] The

*1 Department of Electrical and Material Science
*2 Department of Physics, Faculty of Science, Al-Azhar University, Cairo, Egypt

successful application of LTS diagnostics to micro discharges (secondary streamers) has been reported previously.[20] However, there are two challenges when the LTS method is applied to primary streamers. The first one is that, because of the small Thomson scattering cross-section and the low electron density of the primary streamer (on the order of 10^{18} m^{-3}), the scattering signal level becomes extremely low. The second one is the laser perturbation against the plasma electric state. Because the primary steamer accompanies a very high electric field, the superposition of the strong electromagnetic field in the laser spot may change the electric state in the streamer.

The current investigation aims to solve the above-mentioned problems of the LTS method to diagnose the primary streamer and present the temporal evolution of n_e and T_e in the initial stages of the cathode-directed streamer.

2. Experimental setup and procedure

The electrode set consists of a needle electrode (diameter 1.6 mm) and a hemispherical electrode (diameter 2.4 mm) with a gap distance of 16 mm. These electrodes are made of tungsten and were placed in a vacuum chamber. Power was applied by repeated nanosecond high-voltage pulses with a rise time of 10 ns and a peak voltage of 3 kV. The mono-polar high-voltage pulses were generated by a DC power supply using a fast high-voltage semiconductor switch (BEHLKE HTS50-60) with repetition rate of 10 Hz. The mono-polar pulse generated pulsed discharge in a pure helium gas at pressure of 250 Torr. Our previous research report of the capacity-coupled discharge[20] describes a similar experimental setup and electrical circuit. The polarity of the voltage applied to the needle electrode was positive, so that it led to the formation of a positive streamer moving toward the cathode.

The principles of Thomson scattering diagnostics have been reviewed already, [19),20] and therefore, we only mention that the Thomson scattering in this study is in the incoherent regime and that the scattering is induced by electrons moving independently. The scattered light intensity yields the electron density n_e. The thermal motion of electrons causes the scattered spectrum to be Gaussian due Doppler broadening. Thus, the spread of the scattered spectrum gives the electron temperature T_e.

The light source of the laser Thomson scattering was the second harmonic beam (λ = 532 nm) of a Nd:YAG laser (Continuum, Surelite III). The laser beam (pulse duration of 10 ns, repetition rate of 10 Hz) was focused by a lens and injected in the gap between electrodes inside the chamber. First, a plano-convex lens with focal length of 200 mm was employed to focus the 8mJ laser beam. This setting provided a spot size of 50 μm and a power density of 5×10^{14} W/m^2 and induced the perturbation of the electric state in the streamer. Then, this lens was replaced with a combination of two cylindrical lenses with focal length of 300 mm and 400 mm to avoid laser perturbation. Further explanation of this issue will follow in the next section. The Thomson scattering spectrum was analyzed by a triple-grating spectrometer (TGS) whose configuration, which was designed to reduce the stray light, was almost the same as that used in other experiments.[14)-20] Finally, the spectrum was detected by a gated ICCD camera (Princeton, PI-MAX UNIGEN II).

The propagation of the pulsed streamer was directly observed by the gated ICCD camera, without the TGS. Figure 1 shows the optical emission image of the streamer at different times. In this case, the gated width of the ICCD was set to be 2 ns and the accumulation number was 50.

In order to perform temporally-resolved measurements, the timing of the laser system and ICCD camera, which were synchronized with the laser repetition rate of 10 Hz, were varied with respect to the pulsed discharge using two delay generators (SRS, DG-535). In order to increase the signal-to-noise ratio, the LTS spectrum was accumulated by the ICCD camera over several thousand pulsed discharges and recorded by a computer-based data acquisition system.

3. Results and discussion

Based on the ICCD pictures shown in Fig. 1 and the waveforms of the applied voltage and current shown in Fig. 2, two phases can be observed in the streamer: the primary streamer and the secondary streamer.[12)] At the early stage, the primary steamer formed as a cloud between 0 and 70 ns. The streamer discharge began with an ionization cloud at the tip of the needle electrode (Figs. 1 (a), (b)). The time in Fig.1 (a) is defined as a time origin (t = 0) in this paper. Then, the streamer expanded as a spherical shell toward the

hemispherical electrode at a distance of 16 mm, as shown in Figs. 1 (c) and (d). After that, it reached the hemispherical electrode (Fig. 1 (e)) and finally, by increasing the current, the secondary streamer was created (Fig. 1 (f)). The streamer velocity was calculated to be 10^5 m/s, which is in good agreement with previously reported values.[21)]

The radius of curvature of the needle electrode tip was around 40 μm, and therefore, the electric field intensity when the voltage of 3 kV was applied was estimated to be 8×10^7 V/m. The streamer discharge starts from this point, so in order to observe the effect of the high electric field associated with the steamer, it is desirable to set the observation point as close to the needle tip as possible. However, at a point 1 mm from the needle tip, for example, stray lights produced by needle electrode obstructed signal detection. Finally, we selected a position 2 mm from the needle tip for the Thomson scattering measurement in this paper.

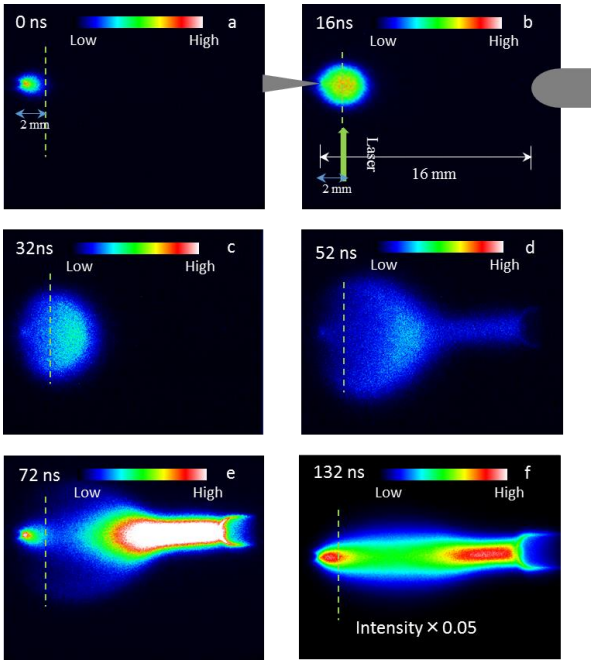

Fig.1 Time evolution of the cathode-directed streamer in helium gas. The images were captured by an ICCD camera. The colors of the images are artificial and show signal intensities. The ICCD camera covered a wavelength range from ultra-violet to near infra-red.

Figure 3 shows an example of the obtained LTS spectrum. The detailed conditions for this spectrum will be described later. In order to keep the signal-to-noise ratio of the measurement sufficiently high, the photon-counting detection technique was employed. The Thomson scattering signals were accumulated by the ICCD camera over 5000 laser shots. It can be seen from Fig. 3 that the measured spectrum is well fitted by a Gaussian curve. Therefore, we can determine the values of n_e and T_e.

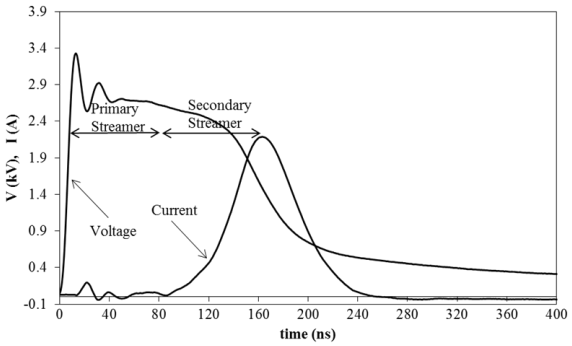

Fig. 2 Voltage and current waveforms.

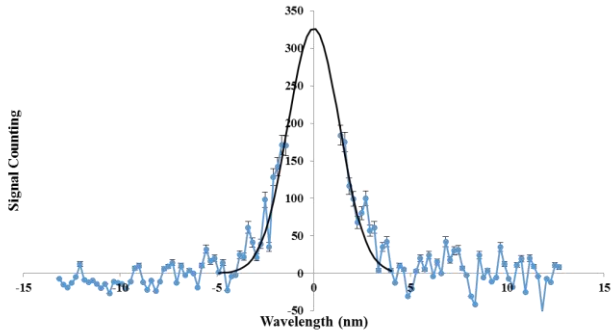

Fig.3 An example of the measured LTS spectrum. The full line is a fitted Gaussian curve.

Since there is a high electric field in the primary streamer particularly near the needle electrode, frequent electron-impact excitations of the gas atoms may occur in this region. Hence, perturbation is possible due to the strong electromagnetic field by the probing laser with a high power density. Yamamoto et al.[22)] reported that the Thomson scattering signal is affected by the photo-ionization of metastable xenon atoms when the laser power density is greater than 10^{15} W/m^2. Chen et al.[23)] also showed that the photo-ionization of metastable argon atoms affects the Thomson scattering spectrum when the power density of the probing laser is greater than 4×10^{13} W/m^2. In the case of the streamer, due to the very high electric field,

the effects of the photo-ionization of all excited atoms must be taken into account. In order to examine the effects of the laser perturbation, the dependence of the signal intensity on the laser power density was investigated. In this investigation, the laser beam focusing system has been changed from a typical plano-convex lens to a combination of two cylindrical lenses whose setup will be shown later. The essential point here is that the beam spot of the probing laser by two cylindrical lenses had a diameter 0.2 mm which is much larger than the 50 μm spot diameter created by the original plano-convex lens. Using the new laser focusing system, the probing laser energy was changed in the range from 10 mJ to 100 mJ. The result is shown in Fig. 4. This measurement was carried out at t = 16 ns when the laser beam hit to the streamer head. The figure shows that the signal intensity is linear up to 1.3×10^{14} W/m^2 and that the signals clearly deviate from the linearity at greater power densities. Therefore, Thomson scattering measurements must be performed below the laser power density of 1×10^{14} W/m^2.

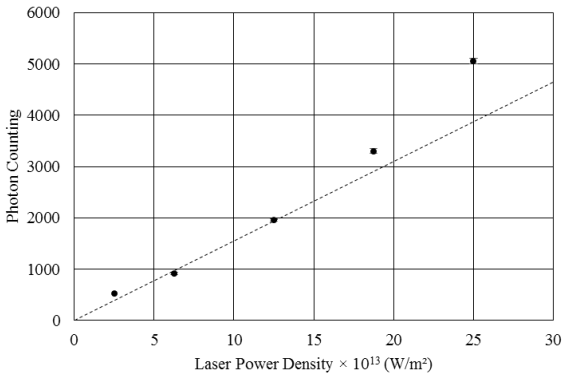

Fig.4 Signal intensity of the Thomson scattering as a function of the laser power density.

Based on above result, we decided to set the laser spot size to be 0.2 mm × 1 mm (so that the actual shape was elliptical) for the further measurements of this study. The setup of the two cylindrical lens system was as illustrated in Fig. 5. As shown in Fig. 1 (b), the laser beam was injected from the lower side of the paper to the upper side. The laser spot size of 0.2 mm was in the direction of the streamer development (left to right). The scattered light was collected using the line of sight perpendicular to the paper surface, and the spot size of 1 mm was in this direction. In order to obtain a clear LTS system, the laser energy was increased up to 100 mJ, which corresponded to a power density of 5×10^{13} W/m^2. This value is well below than the threshold for the laser perturbation. The LTS spectrum shown in Fig. 3 was obtained using this setup.

Figure 6 shows the temporal evolution of n_e and T_e at the point of 2 mm from the needle electrode. At t = 16 ns, the electron temperature was around 2 eV. At this time, the laser beam hit the head of the streamer as shown in Fig. 1 (b). As time passed, T_e decreased to reach a value of 0.83 eV at t = 36 ns. On the other hand, n_e was about 3×10^{18} m^{-3} at this time and subsequently decreased to 1×10^{18} m^{-3} at t = 56 ns. This behavior shows that the electron temperature and electron density have their maximum values at the head of the streamer.

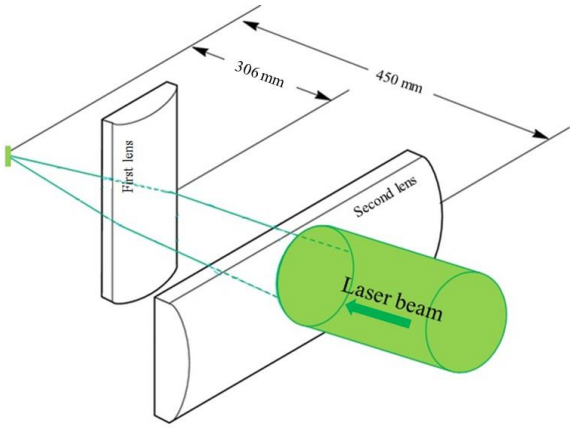

Fig.5 Setup of cylindrical lens system used to shape the laser spot, which measured 1 mm vertically and 0.2 mm horizontally. The axis of the second lens (focal length 400 mm) is perpendicular to that of the first lens (focal length 300 mm).

It has been reported[2] that, in front of the streamer head, the external and internal electric fields combine to make a stronger total field, which boosts ionization. Thus, intense ionization and excitation of gas atoms occur in this region. This could be a strong reason why the light emitted in the streamer head appears in the ICCD images of this experiment (Figs. 1. (b), (c), (d)). On the other hand, inside the streamer and in the plasma channel behind the streamer head, the electric field becomes

weaker, which may slow down the ionization.[21] These features of the streamer are consistent with our observation. Also, the measured values of n_e are close to the simulated helium streamer results at atmospheric pressure in Refs. 21 and 24. At t = 72 ns, the streamer channel reached the hemispherical electrode (Fig. 1 (e)), so the electrical current significantly increase to form a secondary streamer. At this time, T_e and n_e increased dramatically until 140 ns (Figs. 6 (a) and (b)).

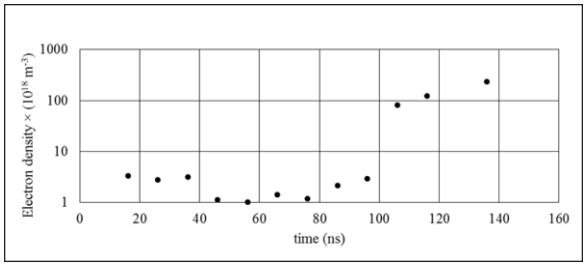

(a)

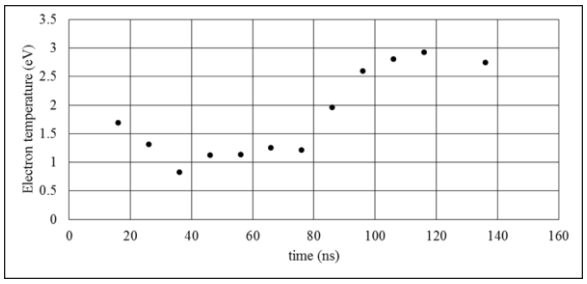

(b)

Fig.6 Temporal evolution of a) electron density and b) electron temperature of the streamer. The measured position is at 2 mm from the needle electrode.

4. Conclusion

In this study, the LTS method was developed to diagnose streamers. In order to avoid laser perturbation, the laser spot size was optimized by using two cylindrical lenses. Because we could utilize a relatively large laser energy without introducing laser perturbation, we could clearly detect LTS signals and measure the n_e and T_e values of the streamer for the first time. Also, measurements of the temporal evolution of n_e and T_e at a point 2 mm from the needle electrode are consistent with reported results from streamer simulations.

References

1) L. B. Loeb and J. M. Meek, the Mechanism of the electric spark (Oxford University Press, Oxford, 1941).
2) M. C. Wang and E. E. Kunhardt, Physical Review A, **42**, 2366 (1990).
3) U. Ebert, W. Saarloos and C. Caroli, Physical review letters, **77**, 4178 (1996).
4) V. F. Tarasneko, Russian Physics Journal, **51**, 656 (2008).
5) V. A. Davidenko, B. A. Dologoshein, and S.V. Somov, Soviet Physics JETP, **28**, 227 (1969).
6) T. M. P. Briels, E. M. van Veldhuizen, and U. Ebert, 15th Int. Conf. Gas Discharges and Their Applications, 2004.
7) T. M. P. Briels, E. M. van Veldhuizen, and U. Ebert, IEEE Trans. on Plasma Science, **33**, 264 (2005).
8) T. M. P. Briels, E. M. van Veldhuizen, and U. Ebert, IEEE Trans. on Plasma Science, **36**, 908 (2008).
9) E. M. van Veldhuizen, S. Nijdam, A. Luque, F. Brau, and U. Ebert, The European Physical Journal Applied Physics, **47**, 2 (2009).
10) Yu. V. Shcherbakov, and L. I. Nekhamkin, Annual Report Conference on Electrical Insulation and Dielectric Phenomena, 2005, p. 593.
11) Y. L. M. Creyghton, Science measurement and technology, IEE Proceedings, **141**, 1994, p 141.
12) R. Ono, and T. Oda, International Journal of Plasma Environmental Science and Technology, **1**, 123 (2007).
13) R. Ono, and T. Oda, Journal of Applied Physics, **97**, 013302 (2005).
14) S. Hassaballa, M. Yakushiji, Y.K. Kim, K. Tomita, K. Uchino, and K. Muraoka, IEEE Trans. Plasma Sci. **32**, 127 (2004).
15) K. Tomita, T. Kagawa, K. Uchino, S. Katsuki, and H. Akiyama, J. Plasma and Fusion Research, **8**, 488 (2009).
16) S. Hassballa, Y. Sonoda, K. Tomita, Y-K. Kim, and K. Uchino, J. Soc. Information Display, **13**, 639 (2005).
17) S. Hassaballa, K. Tomita, Y. K. Kim, K. Uchino, H. Hatanaka, Y. M. Kim, C. H. Park, and K. Muraoka, Jpn. J. Appl. Phys. **44**, L442 (2005).
18) Y. Sonoda, S. Nishimoto, K. Tomita, S. Hassaballa, Y. Yamagata, and K. Uchnio, J. Plasma and Fusion Research, **8**, 696 (2009).
19) K. Tomita, S. Hassballa, and K. Uchino, IEEJ Trans. FM, **130**, 1099 (2010).
20) K. Tomita, N. Bolouki, H. Shirozono, Y. Yamagata, K. Uchino, and K. Takaki, J. Instrum. **7**, C02057 (2012).
21) J-P. Boeuf, L. L. Yang and L. C. Pitchford, J. Phys. D: Appl. Phys. **46**, 015201 (2013).
22) N. Yamamoto, K. Tomita, K. Sugita, T. Kurita, H. Nakashima, and K. Uchino, Review of Scientific Instruments, **83**, 073106 (2012).
23) W. Chen, K. Ogiwara, K. Koge, K. Tomita, K. Uchino, and Y. Kawai, Plasma and Fusion Research, **8**, 1306114 (2013).
24) G. V. Naidis, J. Phys. D: Appl. Phys. **43**, 402001 (2010).